*J. Fluid Mech.* (1990), *vol.* 217, *pp.* 441–467
*Printed in Great Britain*



# Competing and coexisting dynamical states of travelling-wave convection in an annulus

By D. BENSIMON,† PAUL KOLODNER, C. M. SURKO,‡ HUGH WILLIAMS AND V. CROQUETTE†
AT & T Bell Laboratories, Murray Hill, NJ 07974, USA

(Received 16 March 1989 and in revised form 22 January 1990)

We describe experiments on convection in binary fluid mixtures in a large-aspect-ratio annular container. In this geometry, the convective rolls align radially and travel azimuthally, providing a model of travelling waves in an extended one-dimensional nonlinear dynamical system. Several different stable non-equilibrium states can be produced in this experiment, and the competition between them leads to a wide variety of steady and time-dependent behaviour. The observed spatiotemporal behaviour may shed light on recent theories of the nature of stable nonlinear travelling-wave convection, the pinning of travelling waves, and the creation of spatiotemporal defects.

## 1. Introduction

Much recent theoretical work on the subject of chaos and turbulence in fluids has been devoted to the study of models which produce temporally evolving patterns in a single spatial dimension. For example, mechanisms which produce spatiotemporal complexity have been identified in the Kuramoto-Sivashinsky equation and modifications of it (Kuramoto 1978; Sivashinsky 1977, 1979; Shraiman 1986; Chaté & Manneville 1987), as well as in equations of the Ginzburg–Landau type (Nozaki & Bekki 1983; Coullet, Elphick & Repaux 1987). An important goal of our research is to find an experimental system in which the concepts of one-dimensional pattern evolution can be tested. As a first step towards this goal, we report here on observations of the basic states of such a system, as well as on the behaviour of the spatiotemporal defects to which it is susceptible.

Experimental systems displaying complex spatiotemporal behaviour in two and three dimensions abound (Hohenberg & Cross 1987). One of the best known of these model systems is Rayleigh–Bénard convection, in which a thin, horizontal layer of a pure fluid is heated from below. In the last few years, convection in *binary* fluids has also attracted a great deal of interest, because the first instability of the conductive state in this system can be oscillatory (Hurle & Jakeman 1971; Platten & Chavepeyer 1973; Caldwell 1974; Platten & Legros 1984), leading to the existence near onset of dynamical states which have a simple spatial structure (Kolodner *et al.* 1986; Surko & Kolodner 1987). In the parameter range explored in the present paper, this instability triggers a strongly hysteretic transition to a nonlinear state of travelling-wave convection, and complex spatiotemporal behaviour is exhibited in this nonlinear regime (Walden *et al.* 1985; Kolodner *et al.* 1987*a*; Steinberg, Moses &

† Present address: Ecole Normale Supérieure, 24, rue Lhomond, 75231 Paris, France.
‡ Present address: Department of Physics and Institute for Nonlinear Science, University of California at San Diego, La Jolla, CA 92093, USA.

Fineberg 1987). This complexity is observed close to the onset of convection, and so one of the attractions of this system is that this behaviour occurs in a regime which may be theoretically accessible (Brand, Hohenberg & Steinberg 1984; Brand & Steinberg 1984). However, it has not been possible to avoid complicated three-dimensional behaviour in experiments using large-aspect-ratio rectangular cells (Walden *et al.* 1985; Steinberg *et al.* 1987; Kolodner *et al.* 1987*a*), possibly because uniform nonlinear waves in this system may be unstable to the transverse Benjamin–Feir instability (Bretherton & Spiegel 1983; Brand, Lomdahl & Newell 1986). Thus, experiments on convection in wide rectangular cells have not been useful for testing the predictions of one-dimensional models which produce complex behaviour.

One obvious method to suppress higher-dimensional behaviour in convection in rectangular containers is to use narrow convection cells. In such a geometry, it is reasonable to expect that the strongly nonlinear states will consist of straight rolls which propagate parallel to the long side of the cell. However, it is by now well known that propagating rolls can reflect from the short walls of the cell, and it is not understood what consequences these reflections – not to mention more subtle possible effects of the endwalls – might have for the dynamics of complicated nonlinear states. Therefore, we have chosen to conduct experiments in a large-aspect-ratio annular container. In this geometry, the convective pattern is one-dimensional. The rolls are radial, with no transverse structure, and they travel azimuthally. There are no endwalls in the azimuthal direction, and so there are no endwall reflections. It is possible to make a convection cell with mean circumference of greater than 100 times the cell height. The convection pattern in an annular cell satisfies periodic boundary conditions, a case which is often considered in numerical simulations of model equations mentioned previously.

In these experiments, we observe a variety of steady and time-dependent behaviour. This system supports at least three distinct dynamical states in addition to the conductive state: neutrally stable, transient, linear travelling waves exactly at the onset of convection; slow 'overturning' convection which is triggered hysteretically by the linear TW instability; and a state of fast travelling rolls which can coexist stably with the conductive state in isolated angular regions of the cell. These states can be produced separately. In addition, we find that the competition between these states can lead to interesting dynamical behaviour, including complicated transients and spatiotemporal defects. The evolution of the flows produced can often be described in terms of the stability and propagation of the fronts which separate different dynamical states. We have found in general that this system exhibits a rich variety of dynamical behaviour which may be expected to shed considerable light on the nature of nonlinear TW convection in one dimension.

The remainder of this paper is organized as follows. We begin with a description of the physics of travelling-wave convection in binary fluid mixtures, followed by a description of the experimental apparatus. We next discuss experimental results concerning states of uniform, slow convective rolls, stable confined states of fast travelling rolls, transient states, and then spatiotemporal defects. Finally, the significance of the experimental results is considered in the discussion section.

## 2. Travelling-wave convection in binary fluid mixtures

The state of a thin, horizontal layer of a binary fluid mixture which is heated from below can be described by four parameters (Hurle & Jakeman 1971; Platten &

Legros 1984): the Rayleigh number $R$ which is proportional to the applied vertical temperature difference; the Prandtl number $P = \nu/\kappa$ ($\nu$ is the kinematic viscosity, and $\kappa$ is the thermal diffusivity); the Lewis number $L = D/\kappa$ ($D$ is the mass-diffusion coefficient); and the separation ratio $\psi$, which is defined as

$$\psi = -\frac{\partial\rho/\partial c}{\partial\rho/\partial T} c(1-c) S_T. \tag{1}$$

Here, $S_T$ is the Soret coefficient (Kolodner, Williams & Moe 1988*c*). The quantity $\psi$ parametrizes the extent to which Soret-driven concentration diffusion changes the net vertical density gradient.

For $\psi \lesssim -L^2$ and $L \ll 1$, the conductive state loses stability to oscillations when the Rayleigh number is increased above a certain threshold value denoted $r_{co}$. (In this paper, all Rayleigh numbers are normalized to the threshold $R_c = 1707.8$ for the onset of convection in a pure fluid with the same thermal properties as the mixture.) The threshold $r_{co}$ and the linear oscillation frequency $\omega_o$ are now very well understood, both theoretically (Linz & Lücke 1987; Zielinska & Brand 1987; Cross & Kim 1988; Knobloch & Moore 1988) and experimentally (Kolodner *et al.* 1986, 1987*b*, 1988*b*; Surko & Kolodner 1987).

The oscillatory instability is caused by the competition between two diffusion processes – those of heat and of mass – which act on much different timescales when $L \ll 1$. The physical nature of this instability is easy to appreciate if one considers the behaviour of a fluid element which is displaced vertically in an otherwise motionless fluid at a Rayleigh number near threshold. In this situation, a vertical concentration gradient, $\nabla c$, is established by the Soret effect, and the net density gradient, which is proportional to $\psi$, is such that the fluid layer is stable against steady convection in the form of rolls. In the case of small Lewis number, when a fluid element is displaced vertically, it can come to thermal equilibrium with its new surroundings, but its concentration cannot change on the timescale of typical fluid motions. Thus, a displaced fluid element will retain a difference in concentration with its new surroundings and will therefore feel a restoring force due to the resulting density difference. This restoring force, which is proportional to $\psi$, results in oscillations at a frequency which is proportional to $|\psi|^{\frac{1}{2}}$ for small $|\psi|$.

The linear oscillations due to the first instability of the conductive state take the form of travelling waves (Kolodner *et al.* 1986; Surko & Kolodner 1987). In a rectangular convection cell, the wavefronts align parallel to the short side of the cell, propagate parallel to the long side, and reflect from the short endwalls. The travelling waves exhibit a spatial growth rate which depends linearly on the distance above onset, $\epsilon = (r - r_{co})/r_{co}$. We observe that these linear waves do not exhibit nonlinear saturation at small amplitudes for the range of parameters explored in this paper. Rather, their amplitude can be made neutrally stable only by setting the Rayleigh number just enough above onset that the linear growth in space just balances the loss upon reflection from the walls (Cross 1986). In this way, the linear oscillatory transients can be observed for arbitrarily long periods.

If the Rayleigh number is increased above the point of neutral stability, the linear waves will grow and evolve into a nonlinear state. For the values of $\psi$ considered here, this transition is strongly hysteretic, and the resulting nonlinear state, which also consists of travelling waves, is observed to have a much lower oscillation frequency than the linear state seen at onset. Both of these features result from the strong effect of the flow on the background vertical concentration gradient $\nabla c$. When the amplitude of the convection becomes large, the fluid is mixed by the flow, and

$\nabla c$ is reduced from the diffusive profile produced by the Soret effect in the conductive state found below onset. Since $\nabla c$ is the 'spring' which provides the restoring force for the linear oscillations, their frequency drops. Once the travelling waves evolve into a fully nonlinear state, advection by the flow is too strong to be balanced by diffusion, in the regime where $L \ll 1$. This results in the formation of thin boundary layers at the horizontal surfaces of the cell. In this state, the Rayleigh number must be substantially reduced before the advection in the flow is weak enough to be balanced again by diffusion. This is the cause of the strong hysteresis.

A number of experimental observations have been made of this strongly nonlinear state, which we have called 'overturning' convection (Walden *et al.* 1985; Steinberg *et al.* 1987; Kolodner *et al.* 1987*a*). A characteristic feature seen in wide rectangular cells is a pronounced three-dimensional character. It is possible that this is due to a transverse breakup of the travelling waves caused by the Benjamin–Feir instability (Bretherton & Spiegel 1983; Brand *et al.* 1986). The difficulties inherent in characterizing and understanding these three-dimensional flows have been a major factor in our decision to investigate travelling-wave convection in a one-dimensional geometry.

One-dimensional patterns of nonlinear travelling-wave convection in a rectangular geometry have already shown promise of representing an interesting dynamical system. Ahlers, Cannell & Heinrichs (1987), Heinrichs, Ahlers & Cannell (1987), and Moses, Fineberg & Steinberg (1987) have reported the observation of steady 'confined states', in which waves travel towards one of the short walls of the cell and fill only the half of the cell that is bounded by that wall. Cross (1986) has pointed out that such observations can be caused by the convective nature of the instability to travelling waves. By this it is meant that, because the propagation of the waves is in some sense fast compared to the linear growth rate, a local disturbance is carried away by the flow faster than it can grow up locally. This leads to patterns in which the amplitude of convection increases from a small value, measured on one side of the cell, to a saturated nonlinear value, measured on the other side of the cell, as one moves in the direction of propagation of the waves. These states have also been observed to exhibit complicated dynamical behaviour as well (Fineberg, Moses & Steinberg 1988; Kolodner & Surko 1988; Kolodner, Surko & Williams 1989; Steinberg *et al.* 1989). However, Cross' work suggests that endwall reflections are important in producing states exhibiting spatial confinement (Cross 1986, 1988). Thus, it is likely that these observations do not represent the behaviour of travelling-wave convection in an unbounded, one-dimensional geometry. To model an unbounded system, we have therefore been led to conduct the present experiments in an annular convection cell.

## 3. Experimental apparatus and procedure

Figure 1 is a sketch of the apparatus, which we refer to as Cell A, used for most of these experiments. The horizontal boundaries of the convection cell are a rhodium-plated copper mirror on the bottom and a sapphire window on the top. The mirror is heated from below, and the window is cooled from above by circulating water whose temperature is fixed at 24.2 °C. The temperature difference, $\Delta T$, applied across the cell is measured by thermistors in thermal contact with the upper and lower plates. $\Delta T$ is typically 6 °C to 8 °C and is regulated with a stability of $\pm 5 \times 10^{-4}$ °C. A quartz window above the cooling-water channel allows visualization of the convective flow from above by shadowgraphy. The vertical walls of the cell are

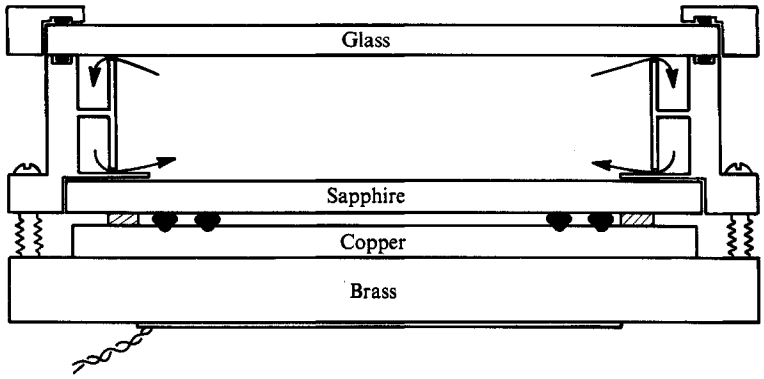


FIGURE 1. Section of the experimental cell referred to as Cell A. The fluid is contained between two concentric o-rings which are sandwiched between a mirror-polished copper bottom plate and a sapphire top plate. Glass spacers just outside the outer o-ring accurately set the gap between the upper and lower plates. The copper mirror is supported by a thick brass plate, to the underside of which is glued an electrical heater. Cooling water circulates above the sapphire top plate. This water is injected into the lower channel of the support structure, sprays out onto the top surface of the sapphire, and is removed from above into the upper channel of the support structure. This assembly is surrounded by low-density polyurethane foam for thermal isolation. Not shown is the magnetic stirring bar which is spun in the cooling water above the sapphire plate in some of the experimental runs.

defined by two ethylene–propylene o-rings which are seated in concentric circular grooves in the bottom plate of the cell. The height of the cell is set at $d = 0.241$ cm by four polished glass spacer tablets which are clamped between the upper and lower plates outside the outer o-ring. The inner and outer diameters of the fluid space between the o-rings are 7.68 cm and 8.47 cm, respectively; thus, the radial aspect ratio of the cell, given by the ratio of the radial width divided by the cell height, is $\Gamma_r = 1.63$, and the circumferential aspect ratio (mean circumference divided by height) is $\Gamma_\phi = 105.3$.

In some of our experiments, we wished to study the effect of a lateral endwall on the flow in the cell. This was done by placing a small piece of o-ring material between the inner and outer o-rings at one location in the cell before clamping it together. The wall filled about 5° of the circumference of the cell. While the wall tended to butt against the inner and outer o-rings and thus to present a severe restriction against flow in the azimuthal direction, no particular attempt was made to make the wall leak-tight.

In several of the experiments reported in this paper, it has been of the utmost importance to ensure that the cell exhibits the best possible azimuthal homogeneity. This is to avoid the existence of places in the cell where local thermal or geometric imperfections can nucleate convection or pin travelling convective rolls. In order to fabricate a cell with uniform height, the apparatus was adjusted in an interferometer during assembly. In some runs, the spatial uniformity of the cell height was better than $\pm 0.05\%$. To ensure uniform cooling of the upper plate of the cell, the cooling water was injected tangentially at the edge of the sapphire plate and caused to circulate azimuthally. In some runs, this circulation was enhanced by spinning a magnetic stirring bar in the centre of the flow channel, driven by a magnet which rotates underneath the lower plate of the cell. In order to eliminate disturbances of the flow caused by filling holes in the walls of the cell, fluid was injected into the cell

through hypodermic needles which were pinched between the o-rings and the sapphire plate before the final assembly of the cell. After filling, these needles were withdrawn, leaving no imperfections to affect the flow.

As noted below, it appears that the onset of oscillatory convection is suppressed by an amount which depends strongly on the radial aspect ratio $\Gamma_r$ of the cell. The o-ring walls of Cell A, while seated in concentric grooves, could not always be clamped down perfectly concentrically every time the cell was dismounted and reassembled. In angular regions where the cell width is narrower, the local Rayleigh number is effectively higher because of the dependence of the instability threshold $r_{co}$ on $\Gamma_r$. Thus, some of the experimental behaviour seen in uniform states of travelling-wave convection, observed at the end of the life of the apparatus, is attributable to non-uniformities in the cell, and these results are not discussed extensively in this paper. To assess and control such effects, the inner o-ring was replaced in some runs with a solid plastic disc with a vertical edge, and additional experiments were carried out in a second cell, referred to as Cell B, whose vertical boundaries were formed by accurately concentric plastic rings. The aspect ratios of Cell B are 1:1.28:66.2, with $d = 0.313$ cm.

One final possible cause of azimuthal asymmetry is the presence of large-scale lateral concentration gradients due to mass transport by travelling convective rolls (Moses & Steinberg 1988). Compositional differences at different locations in the cell result in different values of the fluid parameters and, hence, in different local values of $r_{co}$. Thus, in the presence of such a lateral concentration gradient, even if the vertical temperature difference is applied uniformly, the fluid in different regions of the cell behaves as if it were at different Rayleigh numbers with respect to onset. Such lateral concentration gradients are much more difficult to remove than to produce, since the lateral concentration diffusion time for this cell is several months. In order to avoid these problems, we typically stir the fluid overnight or for several days before each new run by applying a large vertical temperature difference across the cell and allowing a pattern of steady convective rolls to uniformly fill the cell. In this state, convection enhances the mass diffusion by a factor of about 25 (Solomon & Gollub 1988), leading to a homogenization of the fluid in a more reasonable length of time. Moses & Steinberg (1986) have reported the observation of large-scale composition gradients produced by mass transport in the travelling-wave state, as well as their removal by this technique. No evidence has been seen in the present experiments of inhomogeneities caused by lateral composition gradients.

The principal diagnostic technique in these experiments was flow visualization from above by shadowgraphy. The afocal optical system follows the design of Croquette (1989) and is illuminated by a 6-W white light bulb. The image produced by this system is divided by a beamsplitter. One channel is viewed by a 35-mm camera for photography of the flow patterns or by a video camera for monitoring and recording on time-lapse video tape. The other channel is viewed by an EG&G Reticon model CC130 self-scanned annular photodiode array under the control of an AT&T PC 6300 computer. The annular camera has 720 elements and produces a one-dimensional plot of the optical intensity versus azimuthal position in the cell. It is often useful to reduce this data by recording only the positions of the peaks in this plot, which correspond to the downflow roll boundaries in the flow pattern at the instant the image was acquired. By representing these peaks as points arrayed as a function of position along a horizontal line, and by plotting the data from successive instants on lines which are displaced vertically, we can produce a space–time representation of the flow pattern (see figures 3, 6, and 9–15 below). The annular

photodiode array can also be moved along the optical axis into a region of very weak contrast, in which the amplitude of the optical signal is proportional to the focalization distance. In this regime, a linear measurement of the convection amplitude can be made. In the optical system of Cell B, a photomultiplier has been added to record the optical intensity at a single spatial point in the flow-visualization image. This signal is extremely useful for monitoring and stabilizing the flows generated very close to onset, in the same manner as in our previous experiments on linear states in rectangular cells.

The fluid used in these experiments is an 8 wt-% solution of ethyl alcohol in water. In Cell A, where most of the experiments in this paper were performed, the mean temperature of the fluid varied from 28.3 °C to 28.6 °C, depending on the temperature difference applied across the cell. For this solution, $P = 8.91 \pm 0.03$, $L = 0.0084 \pm 0.0001$, and $\psi = -0.248 \pm 0.006$ (Kolodner *et al.* 1988*c*). The vertical thermal diffusion time for this fluid is $\tau_v = d^2/\kappa = 45.1$ s in Cell A. The fluid parameters for experiments in Cell B are similar.

## 4. Experimental results

### 4.1. *Linear waves*

As in rectangular cells, convection in an annulus is triggered by the linear oscillatory instability. While our observations of linear travelling waves in an annulus have been limited, they are in general accord with the extensive study we have made in rectangular cells (Kolodner *et al.* 1986, 1987*b*, 1988*b*; Surko & Kolodner 1987). The first aspect that we can measure is the transition Rayleigh number. In Cell A, we have searched for onset with rather low precision, without recording the wavenumber of the roll pattern, and we find $r_{co} = 1.504 \pm 0.035$. In Cell B, care was taken to stabilize the linear oscillations and to accurately measure their onset Rayleigh number and wavenumber. We measured $r_{co} = 1.702 \pm 0.012$ for a wavenumber $k = 3.322$ for Cell B. These measurements are substantially higher than the values calculated for a laterally infinite system (Cross & Kim 1988): $r_{co} = 1.326 \pm 0.005$ at the critical wavenumber in Cell A, and $r_{co} = 1.354 \pm 0.004$ at the measured wavenumber in Cell B. In a rectangular cell of length $\Gamma_\phi$, a small suppression of the onset, of order $\Gamma_\phi^{-1}$, is caused by the loss in wave amplitude upon reflection from the sidewalls (Kolodner *et al.* 1986). In an annulus, where there is no such loss, even this small effect should be absent. The explanation of the discrepancy may be the same as in pure fluids. In that case, it is well known that the onset of convection is strongly suppressed when the lateral dimension of the cell perpendicular to the roll axes is very small (Catton 1972; Walden *et al.* 1987). Catton (1972) calculates that the onset of convection in a pure fluid in a long, narrow rectangle of width $\Gamma_r$ is suppressed by a factor $1 + (1/2\Gamma_r^{1.75})$. Applying this correction to the theoretical values of $r_{co}$ produces values that are higher than the measured ones by factors $1.069 \pm 0.025$ for Cell A and $1.055 \pm 0.008$ for Cell B. The near equality of these numbers, measured at two different values of $\Gamma_r$, suggests that the transverse width has the same suppression effect on the oscillatory instability as it does on the steady instability in pure fluids.

In Cell B, several runs have been made with the object of stabilizing and characterizing the linear travelling waves. Typically, after the Rayleigh number has been increased just above onset, the photomultiplier signal from a single spatial point in the image of the flow develops growing oscillations which exhibit slow amplitude and frequency modulation. This modulation results from the beating of

several linear modes and can be analysed in the same manner as was done in rectangular cells (Kolodner *et al.* 1988*b*). Because of the sharply wavenumber-dependent linear gain, adjacent modes have different growth rates. Thus, with suitable adjustment of the Rayleigh number, it is possible to cause one mode to have zero growth rate while all the others slowly decay, leaving a unidirectional, single-wavenumber linear wave of time-independent amplitude. This flow can then be allowed to evolve into a nonlinear state by increasing the Rayleigh number. Alternatively, it is possible to abruptly increase the Rayleigh number through the linear onset, producing a linear state of many modes which undergoes a quite different transition to a nonlinear flow. These transients are discussed below.

In extensive measurements of linear mode beating in rectangular cells (Kolodner *et al.* 1988*b*), the frequency splitting between pairs of adjacent resonant modes, as well as the differential growth rates, were used to extract the linear, dispersive parameters of this system. The annular geometry is potentially very useful for making such measurements. One reason for this is that, since an integral number of rolls must fill the cell, the wavenumber of the travelling-wave pattern can be determined with high accuracy directly from Fourier analysis rather than from geometrical measurements, which may be subject to optical distortion. (Because of the phase shift on reflection from the endwalls of a rectangular cell, the number of wavelengths is *not* an integer in that geometry. This makes determination of the precise wavenumber difficult.) Another reason is that, since the circumferential aspect ratio $\Gamma_\phi$ in an annular cell can easily exceed 100, the linear modes are quite closely spaced. Thus, in the cells used in this paper, a single run can exhibit beating between about ten different modes, allowing their growth rates and frequencies to be extracted simultaneously. We have not yet systematically exploited these advantages of the annular geometry in the study of linear travelling-wave convection.

### 4.2. *Uniform states of overturning travelling-wave convection*

When the Rayleigh number is increased above the threshold for the linear instability, the flow evolves, via transients which are discussed below, into a state of uniform overturning convection. As illustrated in the photograph of figure 2, such states consist of an integral number $N$ of convective roll pairs which fill the cell and which propagate in a single direction. Figure 3 shows a space–time representation of such a flow. The number of roll pairs which ultimately develops is a function of the thermal history of the cell. We have been able to produce overturning states with $N = 48$ to 56 roll pairs in Cell A.

Our goal in this experiment has been to study spatiotemporal complexity rather than to fully characterize the basic steady states of this system. Consequently, we did not take particular care to arrange the best geometrical uniformity of the apparatus during this series of experiments. Accordingly, the results in this section will be presented only briefly.

The period $\tau_u$ with which convective rolls travel past a fixed spatial point has been measured for several Rayleigh numbers and mean wavenumbers. The group velocity is always positive and has the value $\partial\omega_u/\partial k_u \sim 0.6$ to 1.6 for typical Rayleigh numbers. The dependence of $\tau_u$ on Rayleigh number is shown for $N = 52$ roll pairs (mean wavenumber $k_u = 3.10$) in figure 4. Below $r \approx 1.52$, the dependence on Rayleigh number is approximately exponential, with a wavenumber-independent slope of $\tau_u^{-1}\partial\tau_u/\partial r = 18$, close to the value $\tau_u^{-1}\partial\tau_u/\partial r = 23$ reported for overturning convection in the same Rayleigh-number range in a rectangular cell at $\psi \sim -0.1$ by Moses & Steinberg (1986). At higher Rayleigh numbers, the period increases even

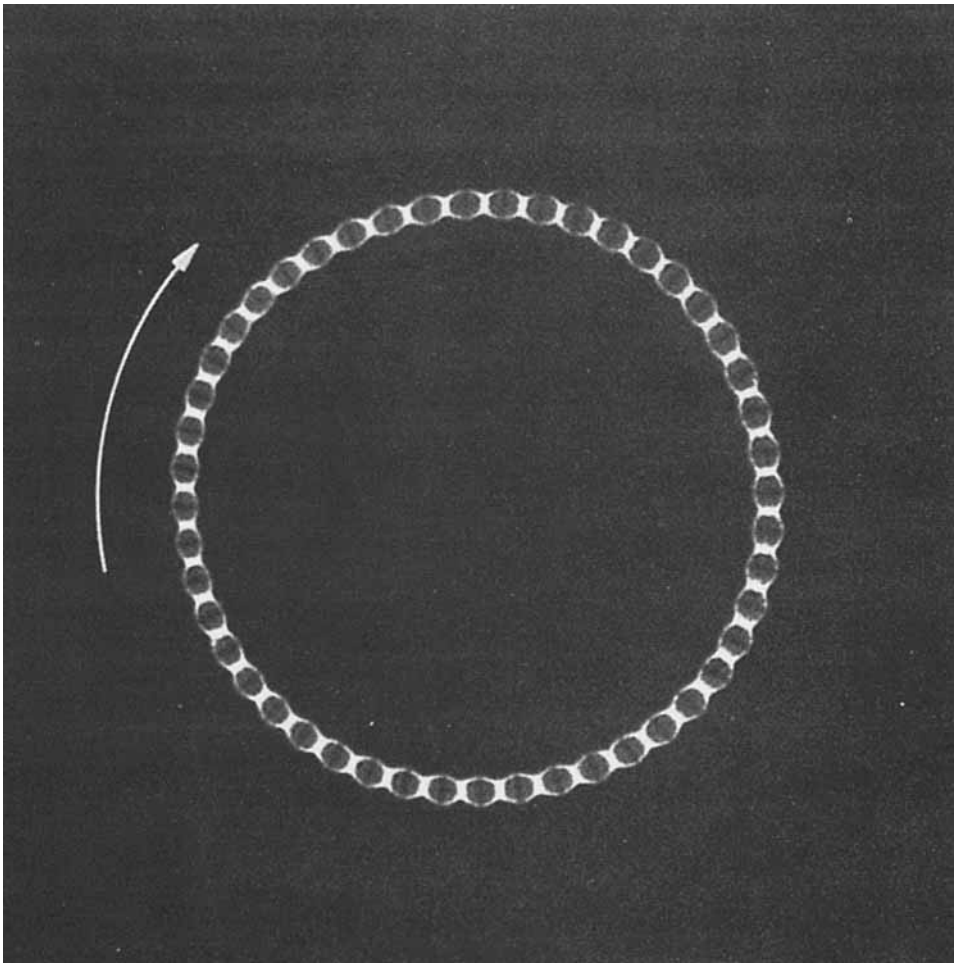

FIGURE 2. Shadowgraph image of a state of uniform, overturning travelling-wave convection in Cell A, at a reduced Rayleigh number $r = 1.52r_{co}$. This state consists of 48 roll pairs which travel clockwise, passing a stationary point with a period $\tau_u = 80\tau_v$.

faster; the overall shape of $\tau_u$ versus $r$ is quite similar to that reported by Moses & Steinberg (1986).† Measurements above $r = 1.54$ made with different $N$ show a great deal of scatter, despite a general increasing trend. The cause of this is unknown, although it should be pointed out that, following a change of Rayleigh number in this range, it can take the better part of a day for $\tau_u$ to settle down to a constant value. For Rayleigh numbers larger than some threshold $r_s \gtrsim 1.6$, the rolls are stationary. It is not known whether $\tau_u$ diverges continuously at $r_s$ or whether the rolls abruptly stop moving upon further increase in $r$, although the work of Moses & Steinberg (1986) suggests the former possibility. These authors, as well as Walden *et al.* (1985), report that the transition back to travelling rolls upon reduction below $r_s$ is hysteretic.

† In our preliminary report of the results in this paper (Kolodner *et al.* 1988*a*), it was stated that the variation of $\tau_u$ with $r$ was much stronger than in rectangular cells. Re-evaluation of our experimental procedure has now made it clear that that statement was based on measurements in which insufficient time was allowed for $\tau_u$ to relax at high Rayleigh numbers.

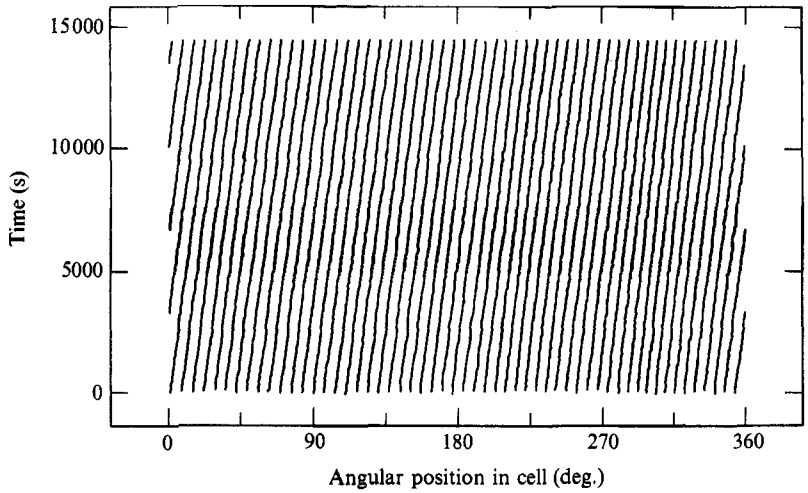


FIGURE 3. Space–time representation of a uniform state like the one in figure 2. Lines mark the positions of downflow roll boundaries (bright stripes in figure 2). Here, the state consists of 55 roll pairs, the Rayleigh number is $r = 1.578 r_{co}$, and the dimensionless oscillation period is $\tau_u = 76\tau_v$.

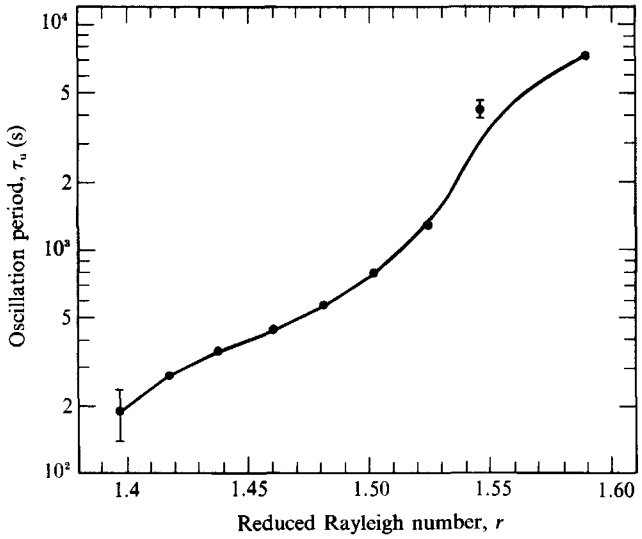


FIGURE 4. Oscillation period $\tau_u$ versus Rayleigh number $r$ for a uniform state of $N = 52$ roll pairs in Cell A. The two error bars represent the standard deviations of the measurements made at those particular Rayleigh numbers. The errors in the rest of the measurements are smaller than the symbols. As discussed in the text, measurements made with different numbers of roll pairs at Rayleigh numbers above $r = 1.54$ exhibit scatter which is greater than the error bars. Thus, the curve has been drawn to match the trend observed in measurements made at several other values of $N$ and misses the point at $r = 1.545$. If the Rayleigh number is reduced below $r \approx 1.4$, the system makes a transition back to the conducting state.

### 4.3. *Confined states*

If we prepare a uniform state and then reduce the Rayleigh number below a certain threshold, then the flow develops a localized conducting region which slowly invades the cell. This process is accompanied by the generation of defects and adjustments of wavenumber and frequency which are described below. The threshold for this

transition depends on the wavenumber of the initial pattern and is found to be about $r = 1.4$ for a pattern of $N = 52$ roll pairs in Cell A. If the Rayleigh number is not increased, this invasion will ultimately lead to a complete transition back to the conducting state. During this phase, the flow consists of two different, spatially separated dynamical states – one conducting, the other convecting – which are separated by sharp boundary regions or fronts. The spatially isolated convecting region is bounded by two fronts, one a trailing edge, from which travelling rolls emerge, and the other a leading edge, towards which the rolls propagate. In a regime where the convecting region is shrinking in space in this way, we define the sum of the velocities of the fronts to be negative.

If the Rayleigh number is increased again before the invasion of the conducting state is complete, then the fronts will slow down. There exists a Rayleigh number above which, in fact, the fronts will reverse, causing the convecting region to invade the cell, producing a uniform state again. There is also an intermediate regime in which the front velocities both vanish exactly, producing a stationary *confined state*. A photograph of such a state is shown in figure 5. The space–time plot shown in figure 6 reveals a number of striking features. First, the front velocities truly vanish. The fronts can remain motionless in this state for days. Second, the roll velocity in this state is much faster than in the uniform states described in the previous section. The oscillation period $\tau_c$ with which confined rolls pass a stationary spatial point is typically $\tau_c = 1.28\tau_v$ in Cell A. This is to be compared with the period $\tau_u = 5.0\tau_v$ to $7.6\tau_v$ measured in the uniform state at the same Rayleigh number, and with the linear period, $\tau_0 = 0.54\tau_v$. A third feature of these confined states is that their wavenumber is quite high – $k_c = 3.64$ in Cell A. The value of $k_c$ decreases perceptibly at the leading edge and increases at the trailing edge. The amplitude $A_c$ of the confined states, as measured by the contrast in the optical image, is comparable with that in the uniform states discussed above: $A_c \approx 1.3A_u$.

A different experimental protocol can be used to produce confined states. As described below, if we start in the conducting state and increase the Rayleigh number abruptly to a value well above the onset $r_{co}$, a spatially complex linear state is produced in which linear waves move in different directions in different parts of the cell. As time proceeds, this linear transient gradually simplifies, evolving into a slow uniform state. If we decrease the Rayleigh number to an appropriate value before this transition is complete, the system can evolve instead to a state in which two or more confined regions exist. A photograph of such a state is shown in figure 7. Typically, different runs will produce different numbers of confined regions which seem to appear in random locations and to have random propagation directions.

A striking observation concerning these confined states is that they have motionless boundaries in a small but finite *band* of Rayleigh numbers. Figure 8 shows that the sum of the leading- and trailing-edge velocities is zero in a band of width $\Delta r = 0.023$ centred at $r = 1.442$. Thus, the front velocities do not simply change sign at some Rayleigh number. Rather, the fronts are truly locked and can remain so for days at a time, at any Rayleigh number within the band, even if $r$ is changed to a different value within the band. If $r$ is increased (decreased) beyond the limits of the band, then the confined convecting regions slowly grow (shrink) and can fill (empty) the entire cell. If the Rayleigh number is moved back into the band before the cell has been filled with or emptied of rolls, we are left again with a stable confined state, and confined regions of any length can apparently be made this way.

The experiments on locked confined regions were conducted under conditions in which we are confident that inhomogeneities play no role. The fact that the period

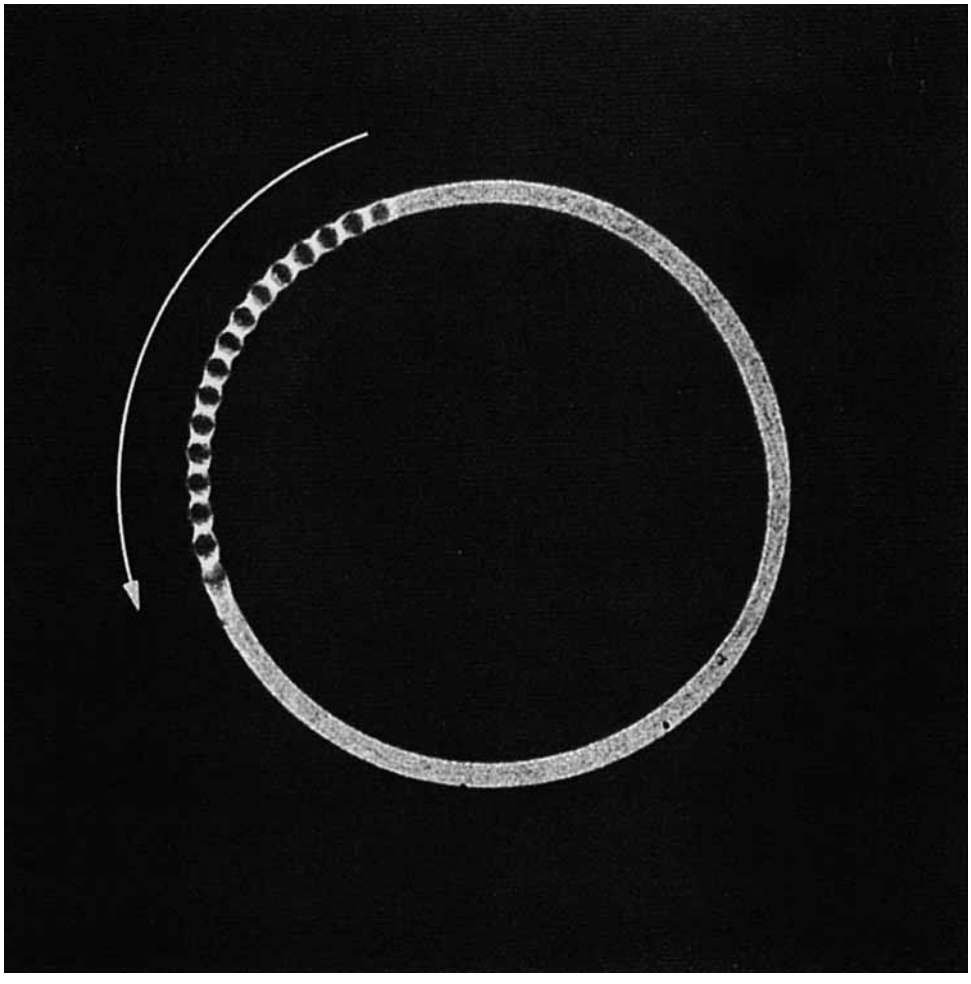

FIGURE 5. Shadowgraph image of a confined state of rolls which travel counterclockwise around Cell A with a period of approximately $\tau_c = 1.28\tau_v$. Note that the roll wavelength is shorter than in the uniform state illustrated in figure 2, and that the wavelength at the leading edge is slightly longer than in the rest of the convecting region.

in the confined state is 5 to 7.6 times faster than the uniform state seen at the same Rayleigh number is a strong indication that this is a different dynamical state entirely, as opposed to simply being a uniform state in which the rolls are pinned to irregularities in the cell. In this series of experiments, the spatial location at which the uniform state developed a conducting region upon reduction of the Rayleigh number appeared to change randomly from run to run, allowing confined states to be produced anywhere in the cell. The length of the confined regions appears not to be fixed, and the propagation direction of the rolls inside the confined regions seems to change randomly from run to run. Finally, uniform states studied around the same time as the experiments on the confined states exhibited only very weak non-uniformities – 2 to 3% – in their wavenumber profiles. These observations suggest that confined regions are not created merely by the presence of some kind of 'weak spot' in the cell.

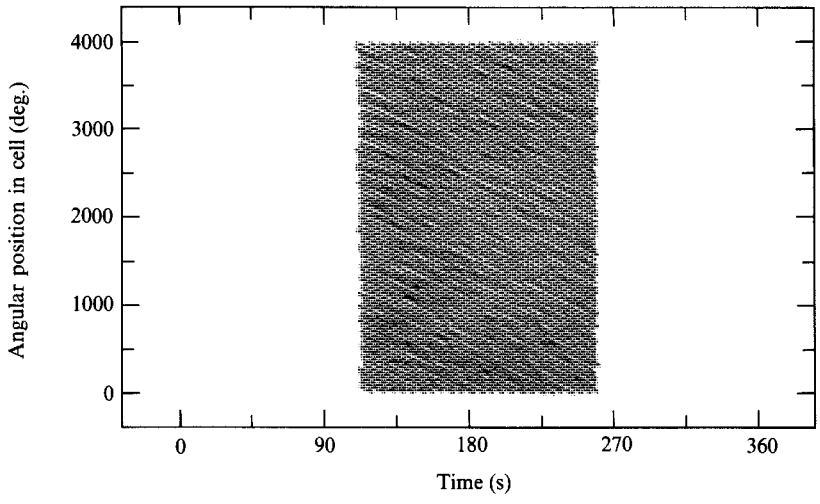


FIGURE 6. Space–time representation of a confined state like that shown in figure 5. Both edges of the confined region are motionless.

Inhomogeneities in the experimental cell could cause other, more subtle, artifacts, including the erroneous observation of a 'locking band'. If in fact there were only a unique Rayleigh number $r_1$ at which the front velocities vanished, rather than a full band, then a large-scale spatial variation of the Rayleigh number could allow the existence of confined rolls over a band of Rayleigh numbers. In this case, if the Rayleigh number varied from below $r_1$ at one side of the cell to above $r_1$ at the other side of the cell, then the boundaries of the convecting region would move to the spatial locations where the local Rayleigh number equals $r_1$ and stop there. The 'confined' rolls would fill the region of the cell where $r > r_1$, and this region would grow (shrink) if the applied temperature difference were increased (decreased). However, we observe no such behaviour. When the Rayleigh number is changed within the band, the locked fronts remain motionless. So it appears that this system can exhibit a true band of locked, confined travelling waves coexisting with regions of conduction.

#### 4.3.1. *Confined states in the presence of an endwall*

As mentioned in §§1 and 5, it is of some importance to understand the connection between the isolated confined states observed in this experiment and the confined states observed in experiments using rectangular cells (Ahlers *et al.* 1987; Heinrichs *et al.* 1987; Moses *et al.* 1987), where the presence of endwalls allows the existence of reflected waves and has a severe impact on the nature of convectively enhanced mass transport (Moses & Steinberg 1988). We therefore made some observations of confined states with an endwall inserted into the channel which forms our cell. In these runs, the confined states could be produced with one front at the wall location, matching observations in rectangular cells. However, confined states in which both the leading and trailing edges were distant from the wall could also be observed.

### 4.4. *Transients*

In our experiments, a wide variety of transient behaviour is observed. Such transients reveal a number of key features of the flow produced in this system. Figure

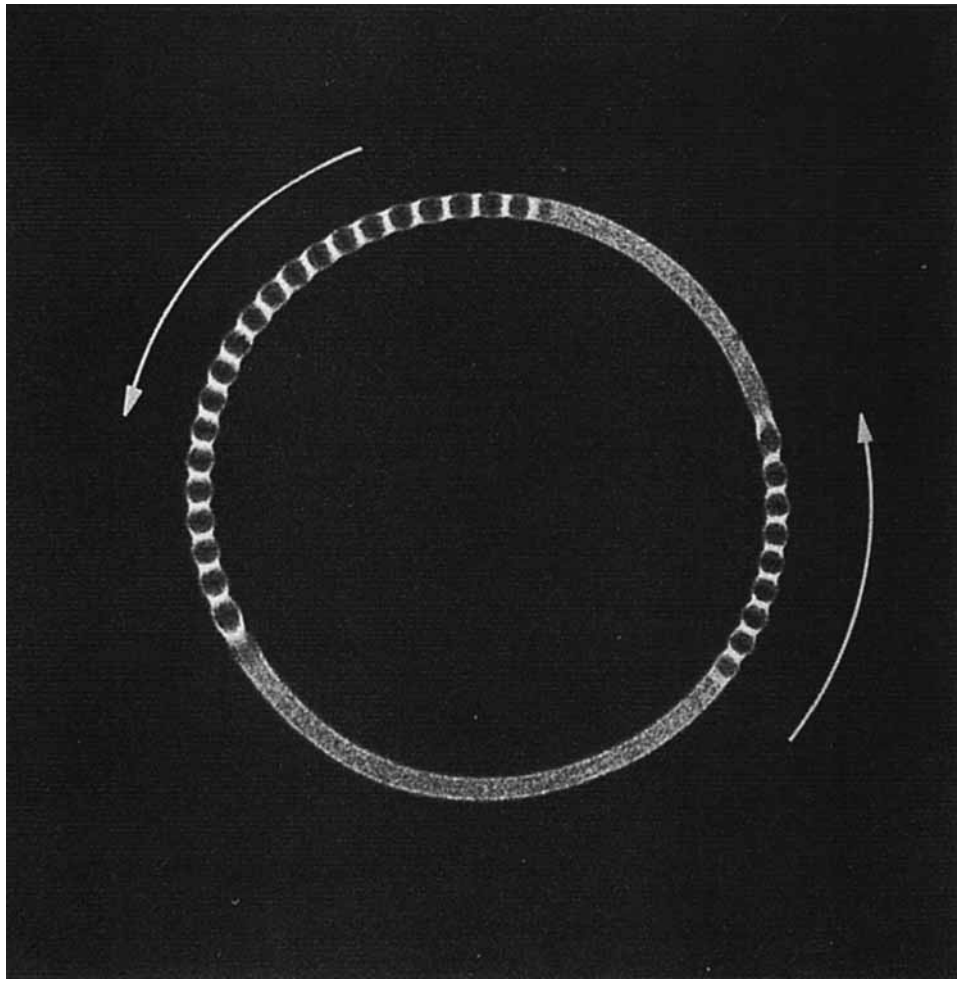

FIGURE 7. Shadowgraph image of a state consisting of two confined regions which happen to travel in the same direction.

9 shows the spatiotemporal behaviour observed in Cell A following a sharp jump through the onset of convection. Initially, the fluid had been held for many hours in a motionless state just below onset ($r_{co} = 1.504$). Then, at time $t = 0$, the Rayleigh number was increased to $r = 1.652$. In the context of our previous studies of linear oscillatory convection (Kolodner *et al.* 1986, 1987*b*, 1988*b*; Surko & Kolodner 1987), this Rayleigh number can be considered far above onset. Because no effort was made during this run to stabilize the linear state and allow modes with wavenumber far from critical to decay, the initial linear flow consists of patches of rolls which move in different directions at different spatial locations. At about $t = 1000$ s, these patches become visible. The subsequent evolution consists of two stages. First, in the time between $t = 1000$ s and $t = 2000$ s, the fast patches 'anneal' and slow down to produce a pattern of rolls which in fact are almost motionless at $t = 2000$ s. (In the next paragraph, we will describe this annealing phase in greater detail.) Second, the slow rolls organize themselves into a uniform state like the ones discussed above. Notice that this uniform state is not the result of the nearly motionless rolls simply

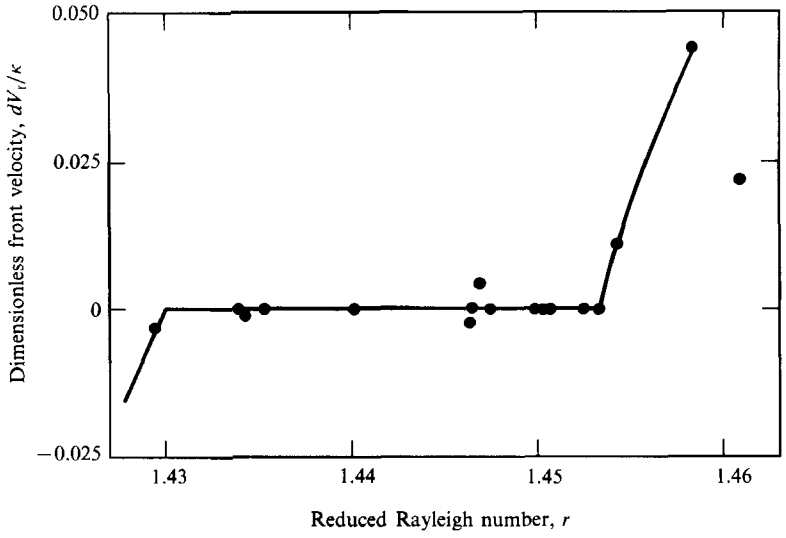


FIGURE 8. The sum of the dimensionless velocities of the leading and trailing edges of confined regions in Cell A is plotted as a function of Rayleigh number. This total front velocity vanishes over a finite band of width $\Delta r = 0.023$ centred at $r = 1.442$. The edges of the band exhibit a slight hysteresis which has not been explored.

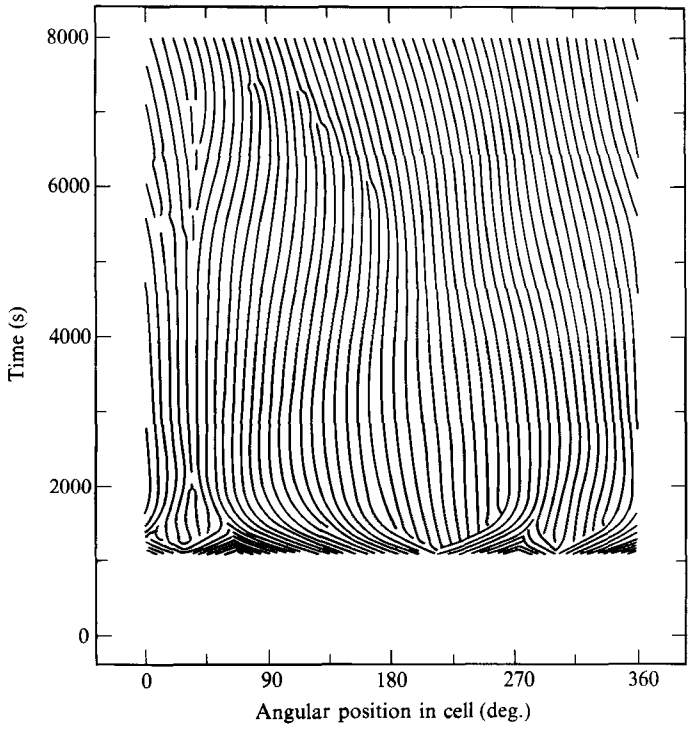


FIGURE 9. Space–time representation of the transient produced in Cell A after the Rayleigh number was jumped from below onset to $r = 1.652$. After about 1000 s, patches of rolls travelling at the linear wave speed appear. These anneal into a system of slow rolls which then evolve into a uniform state by creating space–time dislocations.

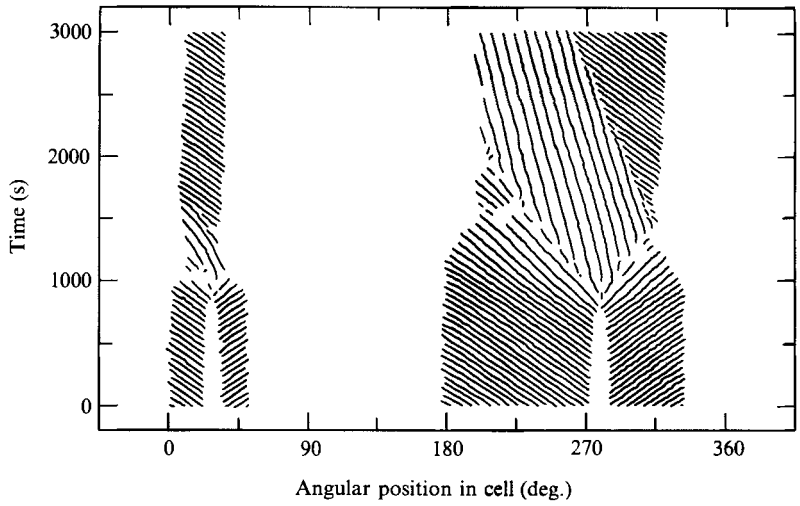


FIGURE 10. Transient produced by creating two neighbouring patches of oppositely propagating confined rolls just above the upper limit of the locking band. The patches expand towards each other and become unstable to slow rolls; these in turn are unstable to fast rolls, which then produce individual patches of confined rolls.

starting to move in one direction or the other. Rather, rolls in different locations start to move in opposite directions, creating a number of 'space–time dislocations' (e.g. at locations 90°–180° from times 6000 s to 7400 s), in which roll pairs are created or destroyed. These defects, which can be produced in a stable way (see §4.5), allow the flow to organize itself into a unidirectional uniform state. At the end of this run, a uniform state with $N = 51$ roll pairs (mean wavenumber $k_u = 3.043$) has evolved.

In the 'annealing' phase mentioned in the last paragraph, neighbouring patches of oppositely propagating linear waves interact to produce slow rolls. We have isolated this process by studying the interaction between oppositely propagating patches of *confined* rolls, as shown in figure 10. In §4.3 on confined states, we described the protocol by which a number of such regions can be produced. To do this, we interrupt a transient like the one shown in figure 9 by decreasing the Rayleigh number to a value in the middle of the locking band during the annealing phase. This prevents the evolution towards a uniform state and instead causes the flow to organize into a small number of spatially separated confined regions. In the run illustrated in figure 10, two pairs of confined patches were thus created. Because the Rayleigh number is in the locking band, these patches can be stabilized for hours and then allowed to interact under controlled conditions. Increasing the Rayleigh number to just above the upper limit of the locking band caused the edges of neighbouring confined regions to expand towards each other. Focusing on the system of rolls centred at location 270° in figure 10, we see that, when the two trailing edges touch, the fast rolls at their intersection become unstable to an expanding set of slow rolls (time $t = 800$ s to 1000 s in figure 10). This fundamental instability is one mechanism by which the annealing in figure 9 produces slow rolls from fast rolls. The other – that is, the production of slow rolls at the intersection of two *leading* edges of fast rolls – is illustrated in figure 11 and is discussed below.

In figure 9, slow rolls are produced by these mechanisms throughout the cell, and their subsequent evolution produces a uniform state. In figure 10, we started with

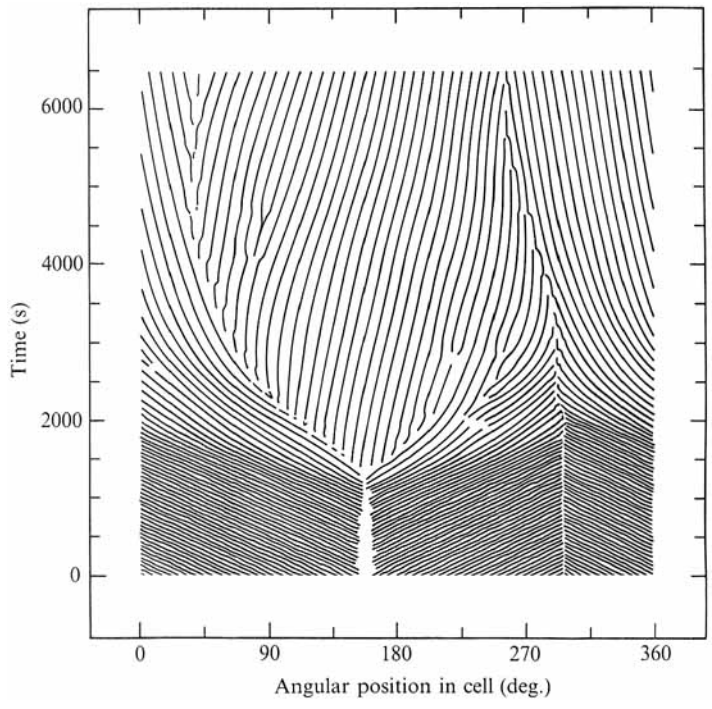


FIGURE 11. Transient evolution of two sets of oppositely propagating rolls travelling at the confined-state speed and separated by a conducting region (location 160°) and a stable sink (location 300°). The flow is destabilized as in figure 10 by the disappearance of the conducting region and evolves towards a uniform state of slow rolls by shedding lines of space–time dislocations in the forms of a slow source and a slow sink which wander through the pattern.

isolated patches of confined rolls, and the interaction of pairs of confined regions initially triggers localized patches of slow rolls. (In the case of figure 10, we refer to the rolls between 201° and 320° at time $t = 1380$ s.) The evolution of such isolated regions of slow rolls provides some insight into the nature of the uniform state. The front at location 200° in figure 10 is a leading-edge interface between slow rolls and the conducting state, and it is observed to be stable. However, the trailing-edge front produced at location 320° at time $t = 1380$ s is unstable. There, fast rolls are nucleated. These invade the slow rolls, ultimately replacing them with a single confined region of fast rolls. Thus we have found a mechanism that prevents the stable existence of confined slow rolls: their trailing edge is unstable to fast rolls. This is consistent with the fact that steady slow rolls are only seen in the uniform state.

Figure 11 illustrates a transient evolution from a system of fast rolls to a uniform state which is complementary to that shown in figure 10. In this run, the initial state exhibited a *sink* – that is, a fixed spatial point where roll pairs are annihilated. In the present case, this defect, seen at location 300° in figure 11, could be termed a fast sink, since the rolls propagate towards it at the speed of confined states. The source of these rolls is a shrinking conduction region at location 160°. The latter structure lost stability to slow rolls at time $t = 1200$ s in much the same way as was seen in figure 10. In parallel with this process, the fast rolls at the sink evolved into slow rolls simply by slowing down, producing a line of space–time dislocations. The resulting complex state of slow rolls again evolved into a unidirectional state by shedding dislocations, as in figure 9. In this case, the lines of dislocations have the appearance

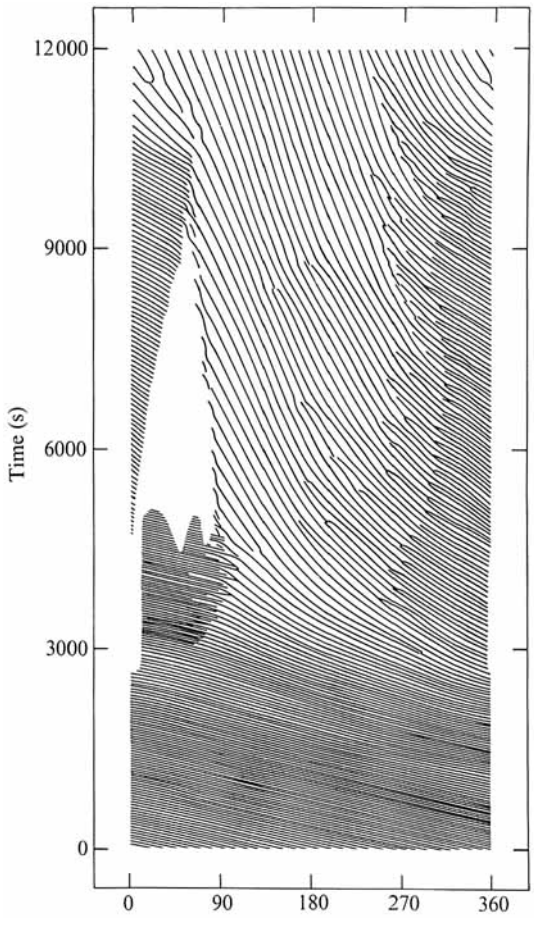


FIGURE 12. Evolution in Cell B of a unidirectional linear state towards a uniform state of slow rolls just above the onset of convection. The transient can be described in terms of the behaviour of fronts between spatially separated regions of different dynamical states.

of source and sink defects which wander slowly through the cell. Ultimately, when all the rolls are moving in the same direction, these defects simply vanish from the pattern, leaving a uniform state.

The discussion in this section has so far centred on the transient evolution of spatially complex states of fast waves. A complementary issue is the fate of a carefully prepared, unidirectional state of linear waves after the Rayleigh number is increased just above onset. Will such waves evolve towards a uniform state simply by slowing down and growing in amplitude, or must this evolution take place in a more complex manner? An answer is provided in figure 12. Here, a unidirectional linear state was stabilized at $r_{co} = 1.702$ for several hours, and then the Rayleigh number was increased to $r = 1.703$. In comparison with the conditions of figure 9, this state is very close to onset.

While the evolution shown in figure 12 is quite complex, the observations of the previous sections allow us to describe it in somewhat simplified terms. Two general features can be noted. First, at any instant in time, the flow consists of different spatial regions, in each of which a different dynamical state is present. For example,

at time $t = 3500$ s, the flow has broken up into four regions: rolls travelling at the speed of confined states (from about 270° to 358°), a conducting region (from 358° to 11°), linear waves (from 11° to about 90°), and slow rolls (from about 90° to about 270°). Second, the evolution of the transient can be largely described in terms of the production of defects and the behaviour of the fronts between the different dynamical states. In previous sections, we learned some of the properties of these fronts. For example, the trailing edge of the rolls which travel at the speed of the confined states (seen at location 358° at time $t = 3500$ s) is seen to expand into the conducting region as time proceeds. This makes sense in terms of the discussion of confined states above. Since the Rayleigh number is well above the locking band, we are in the regime where confined rolls invade neighbouring conducting regions. Likewise, the leading edge of slow rolls (seen at location 90° at time $t = 5000$ s) is almost stable; it expands slowly into the conducting region, and the slow rolls break up in space–time along this front. This behaviour bears some resemblance to the leading-edge fronts of slow rolls seen in figures 10 and 11. There, such fronts were found to be truly stable at one Rayleigh number in the locking band. Clearly, these fronts have a velocity which depends on Rayleigh number.

Some of the fronts seen in figure 12 have not yet been discussed. Between times $t = 3000$ and 4500 s, a front separating fast linear waves from slower rolls is seen near location 90°. Also, after time $t = 3000$ s, a line of space–time dislocations separates confined rolls from slower rolls at about location 270°. This line of dislocations can also be considered as a front and represents a mechanism by which the faster rolls can slow down to produce the fully nonlinear rolls in the uniform state. Below, we shall see that such a line of space–time dislocations can be produced in isolation.

The transient in figure 12 exhibits many similarities to the corresponding transition to finite-amplitude convection in a wide rectangular geometry that was described by Steinberg *et al.* (1987) and by Kolodner *et al.* (1987*a*). Kolodner *et al.* (1987*a*) observed that the principal event consisted of a 'spatial collapse': the evolution from a one-dimensional state of linear travelling waves which filled the cell to a complex, three-dimensional state of overturning convection which was confined to a small region in the centre of the cell. An analogous 'collapse' is seen between time $t = 0$ and $t = 4500$ s in figure 12. Subsequently, the flow in the rectangle evolved by slowly growing to fill the entire cell with an erratic, three-dimensional flow pattern. The same spatial growth is seen in the annulus from $t = 4500$ s to $t = 9000$ s in figure 12. The final phase seen in both geometries is marked by a slowing down of the roll propagation velocity throughout the cell. In the rectangular cell, although the resulting flow remained erratic and three-dimensional, this slowing-down phase was accompanied by the expulsion of defects from the spatial pattern. The line of space–time dislocations seen near location 270° in figure 12 may be the analogue of these real-space defects.

The transient shown in figure 12 demonstrates that, even if the flow begins with a well-defined, spatially simple linear state and evolves to a similarly simple nonlinear state, the evolution in between is by no means uncomplicated. In this system, with its strongly hysteretic transition to overturning convection, the nonlinear state is in fact quite different in character from a simple superposition of linear modes, even in a strictly one-dimensional geometry.

### 4.5. *Stable spatiotemporal defects*

In the previous section, it was clear that spatiotemporal defects – i.e. the localized annihilation and creation of roll pairs – play an important role in the transient

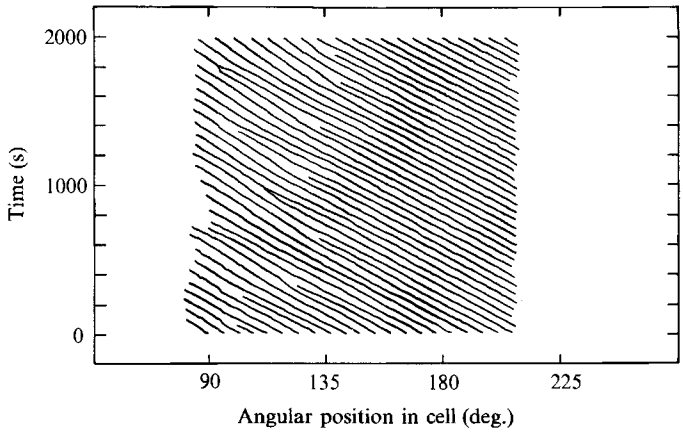


FIGURE 13. Isolated space–time dislocations created near the top of the locking band.

evolution of the flow in this system. Space–time dislocations appeared to have two functions in such transients. First, as shown in figures 9 and 11, dislocations are formed in a pattern of slow rolls which propagate in different directions in different parts of the cell. In this way, the pattern can evolve towards a unidirectional uniform state. Second, as seen in figure 12, dislocations are formed between spatial regions of copropagating rolls which have different velocities. Dislocations form a mechanism by which one dynamical state can spatially evolve into another.

Space–time dislocations can be produced in isolation from other dynamics. In figure 13, an isolated line of dislocations was created when the Rayleigh number was reduced to $r = 1.452$ – i.e. just below the top of the locking band – following a turn-on transient. The rolls on the left-hand side of the figure have a slightly longer wavelength than those on the right. The coexistence of two sets of rolls with different wavelengths is made possible by the repetitive annihilation of roll pairs at a spatial position which fluctuates on timescales on the order of $5\tau_v$ to $10\tau_v$ but which is stable over longer times (i.e. hours). This line of defects may ultimately migrate to the left and disappear, but only on a timescale of many hours to days. Such slow migration is always observed in the direction of the roll propagation. Spatiotemporal dislocations have also recently been observed in nearly one-dimensional travelling-wave patterns in a rectangular geometry at $\psi = -0.058$ by Steinberg *et al.* (1989) and in travelling-wave convection in wide layers of liquid crystals by Joets & Ribotta (1989).

The oscillation period of the rolls on the left-hand side of figure 13 is anomalous: $\tau = 1.67\tau_v$. This is slightly slower than the confined-state period ($\tau_c = 1.21\tau_v$ to $1.28\tau_v$) and 4–6 times faster than the uniform states seen at the same Rayleigh number. The anomalous propagation speed appears to be made possible by the line of space–time dislocations.

The space–time dislocation is a mechanism by which repetitive roll-pair annihilations allow fast rolls to evolve in space to rolls with a slower speed that appears to be selected. The inverse – namely, slow rolls which evolve to fast rolls via repetitive roll-pair creation – is not seen. This would require the existence of a stable trailing-edge front of slow rolls, which we have seen before to be unstable.

A second class of stable defects comprises space–time grain boundaries. An example is the sink of fast rolls observed in figure 11. This defect was destroyed

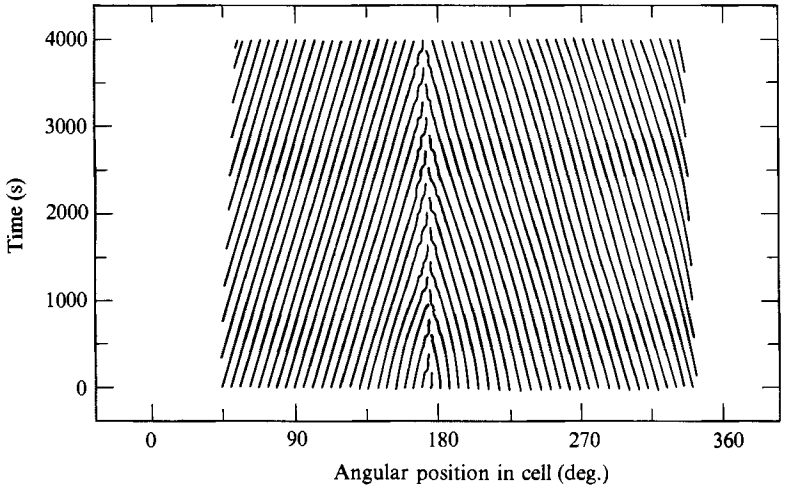


FIGURE 14. Stable sink of slow rolls or 'space–time grain boundary' observed just above onset.

during the disruption of the global pattern by the instability of two intersecting trailing edges of fast rolls. However, the sink had been stationary for the previous 8000 s, and it appears safe to presume that, if the Rayleigh number had been reduced to a value within the locking band during that interval, the fast sink would have been stable indefinitely.

Figure 14 illustrates a *slow* sink which followed a turn-on transient at $r = 1.525$, just above onset. For reasons that we do not understand, the overall spatial extent of the rolls in this run shrank slowly during this run, whose duration was 6 h. Ultimately, the outer trailing edges became unstable to fast rolls which invaded them. However, the sink itself was stable. It is worth noting that the speed of the rolls in this state was anomalous: 2.2 to 4.5 times faster than the uniform states observed at this Rayleigh number.

While the discussion in this section has centred on defects which are stable in the sense that their spatial position is fixed, slowly migrating defects are also important in the evolution of the flow patterns we observe. An example was seen in figure 11, where, after time $t \gtrsim 4000$ s, the flow exhibited a source and a sink defect which wandered slowly through the pattern, allowing the system to find a unidirectional state of slow rolls.

### 4.6. *Defects stabilized by endwalls*

We have seen above that grain boundaries in the form of sinks can be stable in the unbounded annular geometry. However, the formation of *source* defects is a more complicated issue in this system. Attempts to create source defects from patches of outwardly propagating confined rolls always led to transients like those in figures 10 and 11, and stable sources were not created spontaneously during any of the transients we studied. However, when an endwall was installed in the experimental cell, it became possible to observe a stable slow source defect. An example is shown in figure 15. Here, the Rayleigh number was increased from below onset to $r = 1.554$ for 50 min to induce a transition from the conducting state and was then set at $r = 1.443$. The state shown in figure 15 was observed to be stable until the run was terminated 40 h later.

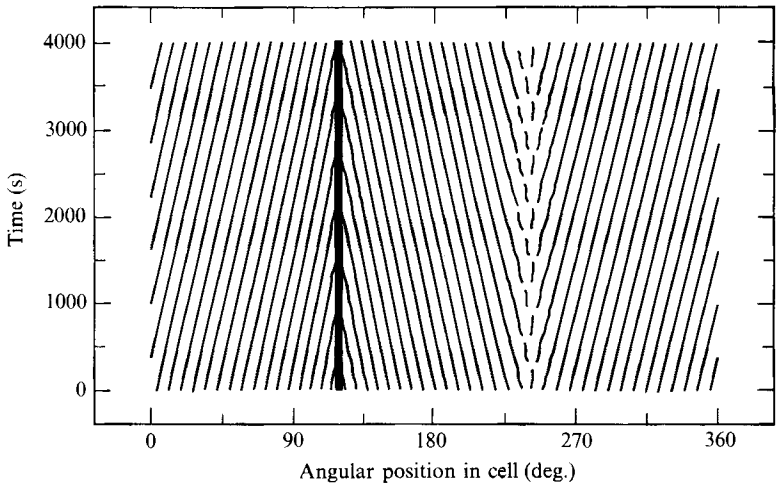


FIGURE 15. Stable source of slow rolls produced at $r = 1.443$ in a cell with a wall. The wall is shown as a solid black bar at location 120°.

## 5. Discussion

Travelling-wave convection in an annulus is a versatile experimental system for exploring a wide variety of complex spatiotemporal behaviour in one dimension. In this paper, we have described the basic non-equilibrium states observable in this system, as well as complicated dynamics due to the interaction between these non-equilibrium states. Some of the behaviour seen in these experiments – specifically, the linear states and uniform overturning states – seem to be analogues of the corresponding states studied previously in rectangular cells. Other behaviour, namely the defects we observe, has not been encountered explicitly in previous experiments. The nature of the fast confined states, by contrast, remains truly mystifying.

The linear oscillatory instability has barely been explored in this geometry. Because of the integral quantization of roll number in the linear modes and the large number of modes which can grow up under the linear gain curve, this system has useful potential in the study of the dispersive properties of linear travelling-wave states. Because this system has no endwalls, the suppression of onset appears to be due solely to the narrow radial aspect ratio. Calculations of this suppression have been performed for the case of steady convection in pure fluids, but not for oscillatory convection in binary mixtures. Experimentally, the threshold Rayleigh number for the onset of an oscillatory flow can be determined much more precisely than that of a steady pattern, because slow drifts in d.c. signal levels do not affect the ability to detect the onset of oscillations. Thus, such measurements could constitute a very stringent test of our quantitative understanding of this effect.

The basic nonlinear state produced in this system consists of slow rolls which uniformly fill the cell and propagate in a single direction. The annular geometry allows these states to be characterized in the absence of reflections from endwalls. Experimentally, it has been quite difficult to produce 'uniform' states in which the wavenumber is truly uniform in space, principally because these states were studied in a cell which had small but noticeable imperfections. Recent progress has been made in improving this aspect by perfecting the geometrical homogeneity of the cell.

Recently, an analysis of nonlinear convection in a horizontally unbounded fluid layer has been performed which, in contrast with previous work, takes into account the existence of concentration boundary layers at the top and bottom horizontal surfaces of the fluid layer (Bensimon, Pumir & Shraiman 1989). The calculation is expected to be quantitatively accurate for $|\psi| \ll 1$ but only qualitatively correct for the parameter values of the present experiments. This calculation predicts that convection is triggered by a subcritical bifurcation from the conductive state. The stable branch of the bifurcation diagram corresponds to a state with thin concentration boundary layers and a slow roll-propagation velocity. This is clearly our 'uniform' state. The calculation predicts the existence of this branch over a range in Rayleigh number of $\delta r \sim 0.1$ for $\psi = -0.25$, which is to be compared with our observed value of $\delta r \sim 0.2$. In the calculation, the roll-propagation velocity is found to decrease with increasing Rayleigh number owing to the sharpening of the boundary layers. For $\psi = -0.25$, the dimensionless oscillation frequency decreases from a maximum of 2.2, at the lowest Rayleigh number, to zero. This is to be compared with our observed maximum uniform-state oscillation frequency of $2\pi\tau_v/\tau_u \sim 1.4$. The calculation also predicts that the transition from this travelling-wave state to steady overturning convection is supercritical. This is at odds with experimental observations made with rectangular cells (Walden *et al.* 1985; Moses & Steinberg 1986), in which steady overturning convection was found to persist hysteretically upon reduction of the Rayleigh number below the transition. However, in a rectangular geometry, the presence of lateral endwalls could stabilize the overturning state against travelling waves, causing this hysteresis. If the calculation is correct, the transition should be supercritical in an annular geometry, where there are no endwalls. This experiment remains to be done.

The bifurcation diagram predicted by the calculations of Bensimon *et al.* (1989) also exhibits an unstable branch which is characterized by a fast propagation velocity and a vertical concentration profile which is quite close to the linear profile produced by the Soret effect in the conducting state. It may be that this branch corresponds to the fast confined state that we observe, and that some aspect of the experiment stabilizes it. A key experimental test of this idea would be to measure the concentration profile in the confined state and compare it with the predictions of the calculation. For the moment, we observe that the calculated amplitude of the unstable branch is somewhat smaller, with respect to the stable branch, than our measured value of $A_c \approx 1.3A_u$.

However, despite this theoretical progress, the true nature of the observed confined states remains a puzzle. While the theory predicts the existence of a state with a fast roll velocity and a weak concentration boundary layer, it does not explain why such a state should be confined, or indeed observable at all. There may in fact be a relationship between the stability and propagation properties of the fronts which bound the confined state and the actual stability of this state. It appears experimentally that leading edges are stable for slow rolls as well as for fast rolls, and possibly for rolls with any speed. Trailing edges, however, are stable only for rolls with the velocity of the confined states. Perhaps the key to understanding these states will be found in the stability properties of such fronts.

Confined states exhibiting a stable trailing-edge front and a high phase velocity have been observed previously in experiments in rectangular containers (Ahlers *et al.* 1987; Heinrichs *et al.* 1987; Moses *et al.* 1987). Stable trailing-edge fronts can be understood in the context of various forms of the Ginzburg–Landau equation as a consequence of the convective nature of the instability to a travelling pattern

(Deissler 1985; Cross 1986; Deissler & Brand 1988). However, such weakly nonlinear models implicitly assume a state of infinitesimal amplitude, so that this understanding may not explain why these fronts remain stable in a system which undergoes a strongly hysteretic transition, such as the one under investigation here. Furthermore, the confined states reported here are the first which exhibit stable leading-edge fronts in the absence of reflections from a wall. The concept of a convective instability does not provide insight into the nature of a leading edge.

Thual & Fauve (1988) have observed that localized pulse-like structures can be stable solutions of a weakly nonlinear dynamical equation which exhibits a subcritical Hopf bifurcation. In this calculation, in which the group velocity is zero, a coupling between the phase and amplitude of the oscillating pattern leads to an effective nonlinear saturation, producing a structure of a fixed shape and length. B. A. Malomed (1988, private communication) has made a similar suggestion. It is not clear what relevance such structures have to our observations. Our confined states are observed in a strongly hysteretic regime, appear to have an arbitrary spatial extent, and are locked in space with respect to the cell, not in the co-moving frame of the rolls. The structures predicted by Thual & Fauve are fixed in the frame of the rolls.

Coullet *et al.* (1987) have suggested that metastable configurations of defects (i.e. leading and trailing edges) may be sustained if there is an oscillatory interaction between such defects. There is no theoretical proof that this is the case for convection in binary fluid mixtures. Their analysis predicts that, the greater the spatial extent of a state confined by this mechanism, the less stable it is (e.g. against changes in temperature). This does not seem to be a characteristic of the confined states we observe.

Bensimon, Shraiman & Croquette (1988), following the suggestion of Pomeau (1986) have proposed that non-adiabatic effects in a system with a weak subcritical bifurcation can cause the locking of fronts to the underlying roll pattern, resulting in confined states that are stable over a small band of Rayleigh numbers in an unbounded, one-dimensional system. It can be demonstrated that such effects can stabilize a front between a conductive region and a region of steady rolls. However, their work suggests that the stabilization of a front of travelling waves requires the existence of a region of standing waves. We have made a preliminary search for such waves at the edges of the confined regions in our experiment. Their amplitude appears to be less than a few percent of that of the dominant wave component.

Finally, Y. Pomeau (1988, private communication) has suggested that confined states are associated with the production of a mean large-scale azimuthal flow. The experiments in which isolated confined states were observed in a cell with an endwall tend to discount this suggestion, although the endwalls we used were not completely leakproof. In this regard, it will be of some interest to conduct the same experiments with a leak-tight endwall, perhaps using the photochromic mass-transport technique of Croquette (1989), Croquette *et al.* (1986), and Moses & Steinberg (1988) as a diagnostic for the presence of such large-scale flows. In the meantime, the first question raised by our observation of confined states – namely, their very existence and the stability of their leading edges – remains unanswered.

The notion of the study of the fronts between dynamical states, as opposed to the examination of the basic non-equilibrium states of the system without fronts or boundaries, becomes important when we consider transients and defects. Indeed, we have adopted a language which describes such behaviour mainly in terms of the stability and propagation of these fronts. For example, we have noted that leading

edges separating travelling rolls from a conducting region appear to be stable at every observed propagation speed. Similarly, the front separating slow rolls from fast rolls which follow them is either roughly stable on short timescales, as in figure 13, or 'invasive', as in the transient illustrated in figure 10. This instability of trailing edges of slow rolls explains why stable states of confined slow rolls are not seen. Of course, this 'explanation' merely defers the question; why such trailing edges are unstable is not known.

Another important comment concerning front properties is that they have been explored in this paper only for one particular fluid concentration. At different values of $\psi$, these fronts between different dynamical states may have different velocities and stability properties, leading to dynamical behaviour that is qualitatively much different from that reported in this paper.

Establishment of fronts between regions containing different dynamical states is a general way in which a system can exhibit complex spatiotemporal behaviour. Defects form an important subset of the family of possible fronts. We have isolated two kinds of stable defects: dislocations and grain boundaries. Concerning the latter, an important question is why sinks of rolls can be stable in an unbounded system while sources appear to be stable only in experiments in which a lateral wall was put in the cell. Dislocations have been found to be a ubiquitous way for accommodating different dynamical states in the same flow. The system of dislocations shown in figure 13, for example, allows a region of flow with one wavenumber to evolve spatially to another wavenumber. In figures 9 and 11, dislocations permit a system of slow rolls travelling with different velocities and directions at different places to select a unique propagation velocity. In general, such mechanisms must play an important role in producing turbulence; that is, complex flows with a wide range of wavenumbers. The study of dislocations is also part of the key to an understanding of the weaker case of one-dimensional phase turbulence.

It is a pleasure to acknowledge useful discussions with P. C. Hohenberg, B. Shraiman and M. C. Cross. We also thank M. C. Cross for providing us with software to calculate properties of the linear oscillatory instability.

## REFERENCES

AHLERS, G., CANNELL, D. S. & HEINRICHS, R. 1987 Convection in a binary mixture. *Nucl. Phys. B (Proc. Suppl.)* **2**, 77–86.

BENSIMON, D., PUMIR, A. & SHRAIMAN, B. I. 1989 Nonlinear theory of traveling wave convection in binary mixtures. *J. Phys. Paris* **50**, 3089–3108.

BENSIMON, D., SHRAIMAN, B. I. & CROQUETTE, V. 1988 Nonadiabatic effects in convection. *Phys. Rev.* **A38**, 5461–5464.

BRAND, H. R., HOHENBERG, P. C. & STEINBERG, V. 1984 Codimension-2 bifurcations for convection in binary fluid mixtures. *Phys. Rev.* **A30**, 2548–2561.

BRAND, H. R., LOMDAHL, P. S. & NEWELL, A. C. 1986 Benjamin–Feir turbulence in convective binary fluid mixtures. *Physica* **23D**, 345–361.

BRAND, H. R. & STEINBERG, V. 1984 Analog of the Benjamin–Feir instability near the onset of convection in binary fluid mixtures. *Phys. Rev.* **A29**, 2303–2304.

BRETHERTON, C. S. & SPIEGEL, E. A. 1983 Intermittency through modulational instability. *Phys. Lett.* **96A**, 152–156.

CALDWELL, D. R. 1974 Experimental studies on the onset of thermohaline convection. *J. Fluid Mech.* **64**, 347–367.

CATTON, I. 1972 The effect of insulating vertical walls on the onset of motion in a fluid heated from below. *J. Heat Mass Transfer* **15**, 665–672.

CHATÉ, H. & MANNEVILLE, P. 1987 Transition to turbulence via spatiotemporal intermittency. *Phys. Rev. Lett.* **58**, 112–115.

COULLET, P., ELPHICK, C. & REPAUX, D. 1987 Nature of spatial chaos. *Phys. Rev. Lett.* **58**, 431–434.

CROQUETTE, V. 1989 Convective pattern dynamics at low Prandtl number: Part I. *Contemp. Phys.* **30**, 113–133.

CROQUETTE, V., LE GAL, P., POCHEAU, A. & GUGLIELMETTI, R. 1986 Large-scale flow characterization in a Rayleigh–Bénard convective pattern. *Europhys. Lett.* **1**, 393–399.

CROSS, M. C. 1986 Traveling and standing waves in binary-fluid convection in finite geometries. *Phys. Rev. Lett.* **57**, 2935–2938.

CROSS, M. C. 1988 Structure of nonlinear traveling-wave states in finite geometries. *Phys. Rev.* **A38**, 3593–3600.

CROSS, M. C. & KIM, K. 1988 Linear instability and the codimension-2 region in binary fluid convection between rigid impermeable boundaries. *Phys. Rev.* **A37**, 3909–3920.

DEISSLER, R. J. 1985 Noise-sustained structure, intermittency, and the Ginzburg–Landau equation. *J. Statist. Phys.* **40**, 371–395.

DEISSLER, R. J. & BRAND, H. R. 1988 Generation of counterpropagating nonlinear interacting traveling waves by localized noise. *Phys. Lett.* **A130**, 293–298.

FINEBERG, J., MOSES, E. & STEINBERG, V. 1988 Spatially and temporally modulated traveling-wave pattern in convecting binary mixtures. *Phys. Rev. Lett.* **61**, 838–841.

HEINRICHS, R., AHLERS, G. & CANNELL, D. S. 1987 Traveling waves and spatial variation in the convection of a binary mixture. *Phys. Rev.* **A35**, 2761–2764.

HOHENBERG, P. C. & CROSS, M. C. 1987 An introduction to pattern formation in nonequilibrium systems. *Fluctuations and Stochastic Phenomena in Condensed Matter* (ed. L. Garrido), pp. 55–92. Springer.

HURLE, D. T. J. & JAKEMAN, E. 1971 Soret-driven thermosolutal convection. *J. Fluid Mech.* **47**, 667–689.

JOETS, A. & RIBOTTA, R. 1989 Localisation and defects in propagative ordered structures. *J. Phys. Paris* **50**, C3/171–C3/180.

KNOBLOCH, E. & MOORE, D. R. 1988 Linear stability of experimental Soret convection. *Phys. Rev.* **A37**, 860–870.

KOLODNER, P., BENSIMON, D. & SURKO, C. M. 1988*a* Traveling-wave convection in an annulus. *Phys. Rev. Lett.* **60**, 1723–1726.

KOLODNER, P., PASSNER, A., SURKO, C. M. & WALDEN, R. W. 1986 Onset of oscillatory convection in a binary fluid mixture. *Phys. Rev. Lett.* **56**, 2621–2624.

KOLODNER, P., PASSNER, A., WILLIAMS, H. L. & SURKO, C. M. 1987*a* The transition to finite-amplitude traveling-wave convection in binary fluid mixtures. *Nucl. Phys. B (Proc. Suppl.)* **2**, 97–108.

KOLODNER, P. & SURKO, C. M. 1988 Weakly nonlinear traveling-wave convection. *Phys. Rev. Lett.* **61**, 842–845.

KOLODNER, P., SURKO, C. M., PASSNER, A. & WILLIAMS, H. L. 1987*b* Pulses of oscillatory convection. *Phys. Rev.* **A36**, 2499–2502.

KOLODNER, P., SURKO, C. M. & WILLIAMS, H. 1989 Dynamics of traveling waves near the onset of convection in binary fluid mixtures. *Physica* **37D**, 319–333.

KOLODNER, P., SURKO, C. M., WILLIAMS, H. L. & PASSNER, A. 1988*b* Two-frequency states at the onset of convection in binary fluid mixtures. In *Propagation in Systems Far from Equilibrium* (ed. J. E. Wesfreid, H. R. Brand, P. Manneville, G. Albinet & N. Boccara), pp. 282–291. Springer.

KOLODNER, P., WILLIAMS, H. & MOE, C. 1988*c* Optical measurement of the Soret coefficient of ethanol/water solutions. *J. Chem. Phys.* **88**, 6512–6524.

KURAMOTO, Y. 1978 Diffusion-induced chaos in reaction systems. *Suppl. Prog. Theor. Phys.* **64**, 346–367.

LINZ, S. J. & LÜCKE, M. 1987 Convection in binary mixtures: a Galerkin model with impermeable boundary conditions. *Phys. Rev.* **A35**, 3997–4000.

MOSES, E., FINEBERG, J. & STEINBERG, V. 1987 Multistability and confined traveling-wave patterns in a convecting binary mixture. *Phys. Rev.* **A35**, 2757–2760.

MOSES, E. & STEINBERG, V. 1986 Flow patterns and nonlinear behavior of traveling waves in a convecting binary fluid. *Phys. Rev.* **A34**, 693–696.

MOSES, E. & STEINBERG, V. 1988 Mass transport in propagating patterns of convection. *Phys. Rev. Lett.* **60**, 2030–2033.

NOZAKI, K. & BEKKI, N. 1983 Pattern selection and spatiotemporal transition to chaos in the Ginzburg–Landau equation. *Phys. Rev. Lett.* **51**, 2171–2174.

PLATTEN, J. K. & CHAVEPEYER, G. 1973 Oscillatory motion in Bénard cell due to the Soret effect. *J. Fluid Mech.* **60**, 305–319.

PLATTEN, J. K. & LEGROS, J. C. 1984 *Convection in Liquids*. Springer.

POMEAU, Y. 1986 Front motion, metastability, and subcritical bifurcations in hydrodynamics. *Physica* **23D**, 3–11.

SHRAIMAN, B. I. 1986 Order, disorder, and phase turbulence. *Phys. Rev. Lett.* **57**, 325–328.

SIVASHINSKY, G. I. 1977 Nonlinear analysis of hydrodynamic instability in laminar flame. I. Derivation of basic equations. *Acta Astronaut.* **4**, 1177–1206.

SIVASHINSKY, G. I. 1979 On self-turbulization of a laminar flame. *Acta Astronaut.* **6**, 569–591.

SOLOMON, T. H. & GOLLUB, J. P. 1988 Passive transport in steady Rayleigh–Bénard convection. *Phys. Fluids* **31**, 1372–1379.

STEINBERG, V., FINEBERG, J., MOSES, E. & REHBERG, I. 1989 Pattern selection and transition to turbulence in propagating waves. *Physica* **37D**, 359–383.

STEINBERG, V., MOSES, E. & FINEBERG, J. 1987 Spatio-temporal complexity at the onset of convection in a binary fluid. *Nucl. Phys. B (Proc. Suppl.)* **2**, 109–123.

SURKO, C. M. & KOLODNER, P. 1987 Oscillatory traveling-wave convection in a finite container. *Phys. Rev. Lett.* **58**, 2055–2058.

THUAL, O. & FAUVE, S. 1988 Localized structures generated by subcritical instabilities. *J. Phys. Paris* **49**, 1829–1832.

WALDEN, R. W., KOLODNER, P., PASSNER, A. & SURKO, C. M. 1985 Traveling waves and chaos in convection in binary fluid mixtures. *Phys. Rev. Lett.* **55**, 496–499.

WALDEN, R. W., KOLODNER, P., PASSNER, A. & SURKO, C. M. 1987 Heat transport by parallel-roll convection in a rectangular container. *J. Fluid Mech.* **185**, 205–233.

ZIELINSKA, B. J. A. & BRAND, H. R. 1987 Exact solution of the linear stability problem for the onset of convection in binary fluid mixtures. *Phys. Rev.* **A35**, 4349–4353.